MRFD Method for Scattering
from Three Dimensional Dielectric Bodies

Ahmet Fazil YAGLI

Turksat A.S. Ar-Ge Uydu Tasarim Dir. Gazi Universitesi Teknopark, Golbasi Ankara, Turkey

afyagli@turksat.com.tr

Abstract. *A three-dimensional multiresolution frequency domain (MRFD) method is established to compute bistatic radar cross sections of arbitrarily shaped dielectric objects. The proposed formulation is successfully verified by computing the bistatic radar cross sections of a dielectric sphere and a dielectric cube. Comparing the results to those obtained from the finite difference frequency domain (FDFD) method simulations and analytic calculations, we demonstrated the computational time and memory advantages of MRFD method.*

Keywords

FDFD method, MRFD method, electromagnetics, scattering.

1. Introduction

Researchers have used the finite difference frequency domain (FDFD) method to solve electromagnetic scattering problems successfully [1–4]. FDFD method presents a mathematically simple and stable way of solving Maxwell's equations, on the other hand, large amount of computer memory and simulation time requirements are its disadvantages. In order to overcome these disadvantages, the multiresolution frequency domain (MRFD) technique was developed [5–8], which needs less computer resources and simulation time than FDFD.

In this study, the MRFD scheme is formulated to model three-dimensional open space problems, particularly scattering from dielectric objects. The scattered field formulation [9] and Berenger's [10] perfectly matched layer (PML) are implemented into the MRFD formulation. The MRFD formulation in this study is based on Cohen-Daube-chies-Feauveau (CDF) family of wavelets [11]. To have an effective MRFD algorithm, the CDF (2,2) wavelet is utilized in this work because of its compact support, symmetry, and regularity [7]. Since the MRFD computation space is truncated, a near field to far field transformation method is also used to obtain the scattered far field [12]. For comparison purposes, we used the exact scattering data of the dielectric objects obtained from the computer program

developed by Demir et al. [13]. The improvement of MRFD method in memory requirement and simulation time is demonstrated.

2. Formulation

The formulation developed in this paper is based on the pure scattered field formulation in which the total field is the sum of the known incident and the unknown scattered fields. This formulation evolves from the linearity of Maxwell's equations and the decomposition of the total electric and magnetic fields into incident and scattered fields.

$$\vec{E}_{total} = \vec{E}_{inc} + \vec{E}_{scat} , \tag{1.a}$$

$$\vec{H}_{total} = \vec{H}_{inc} + \vec{H}_{scat} . \tag{1.b}$$

The incident field is the field that would exist in the computational domain in which no scatterers exist and therefore satisfies the Maxwell's equations as

$$\nabla \times \vec{E}_{inc} = -j\omega\mu_o \vec{H}_{inc} , \tag{2.a}$$

$$\nabla \times \vec{H}_{inc} = +j\omega\varepsilon_o \vec{E}_{inc} . \tag{2.b}$$

The total fields also satisfy the Maxwell's equations by definition

$$\nabla \times \vec{E}_{total} = -j\omega\mu \vec{H}_{total} , \tag{3.a}$$

$$\nabla \times \vec{H}_{total} = +j\omega\varepsilon \vec{E}_{total} . \tag{3.b}$$

Using the scattered field decomposition (1), the curl equations (2 and 3) can be combined to yield

$$\nabla \times \vec{E}_{scat} + j\omega\mu \vec{H}_{scat} = j\omega\left(\mu_o - \mu\right)\vec{H}_{inc} , \tag{4.a}$$

$$\nabla \times \vec{H}_{scat} - j\omega\varepsilon \vec{E}_{scat} = j\omega\left(\varepsilon - \varepsilon_o\right)\vec{E}_{inc} . \tag{4.b}$$

Decomposing the vector equations to x, y, and z components, we obtain six scalar equations as

$$\frac{\partial E_{scat,z}}{\partial y} - \frac{\partial E_{scat,y}}{\partial z} + j\omega\mu_x H_{scat,x} = j\omega\left(\mu_o - \mu_x\right)H_{inc,x}$$

$$\frac{\partial E_{scat,x}}{\partial z} - \frac{\partial E_{scat,z}}{\partial x} + j\omega\mu_y H_{scat,y} = j\omega\left(\mu_o - \mu_y\right)H_{inc,y} \quad (5)$$

$$\frac{\partial E_{scat,y}}{\partial x} - \frac{\partial E_{scat,x}}{\partial y} + j\omega\mu_z H_{scat,z} = j\omega\left(\mu_o - \mu_z\right)H_{inc,z}$$

$$\frac{\partial H_{scat,z}}{\partial y} - \frac{\partial H_{scat,y}}{\partial z} - j\omega\varepsilon_x E_{scat,x} = j\omega\left(\varepsilon_x - \varepsilon_o\right)E_{inc,x}$$

$$\frac{\partial H_{scat,x}}{\partial z} - \frac{\partial H_{scat,z}}{\partial x} - j\omega\varepsilon_y E_{scat,y} = j\omega\left(\varepsilon_y - \varepsilon_o\right)E_{inc,y} \quad (6)$$

$$\frac{\partial H_{scat,y}}{\partial x} - \frac{\partial H_{scat,x}}{\partial y} - j\omega\varepsilon_z E_{scat,z} = j\omega\left(\varepsilon_z - \varepsilon_o\right)E_{inc,z}.$$

The set of equations formed by (5) and (6) is the basis of the MRFD numerical algorithm for electromagnetic wave interactions with arbitrarily shaped dielectric objects.

Since the computational space is truncated, an absorbing boundary condition is established. A perfectly matched layer (PML) for FDTD developed by Berenger [10] to absorb the outgoing waves is utilized in this study. A PML formulation, developed by Kuzu et al. [1], is used to surround the scatterer and terminate the computational space. The subscripts of parameters ε and μ in (5) to (8) are utilized to indicate the anisotropic permittivity and permeability of the PML layer [1], in non-PML region, these parameters are isotropic.

The computational space can be modeled using the equations as [1, 4]

$$H_{scat,x} + \frac{1}{j\omega\mu_{xy}}\frac{\partial E_{scat,z}}{\partial y} - \frac{1}{j\omega\mu_{xz}}\frac{\partial E_{scat,y}}{\partial z} = \frac{\mu_o - \mu_{xi}}{\mu_{xi}}H_{inc,x}$$

$$H_{scat,y} + \frac{1}{j\omega\mu_{yz}}\frac{\partial E_{scat,x}}{\partial z} - \frac{1}{j\omega\mu_{yx}}\frac{\partial E_{scat,z}}{\partial x} = \frac{\mu_o - \mu_{yi}}{\mu_{yi}}H_{inc,y} \quad (7)$$

$$H_{scat,z} + \frac{1}{j\omega\mu_{zx}}\frac{\partial E_{scat,y}}{\partial x} - \frac{1}{j\omega\mu_{zy}}\frac{\partial E_{scat,x}}{\partial y} = \frac{\mu_o - \mu_{zi}}{\mu_{zi}}H_{inc,z}$$

$$E_{scat,x} - \frac{1}{j\omega\varepsilon_{xy}}\frac{\partial H_{scat,z}}{\partial y} + \frac{1}{j\omega\varepsilon_{xz}}\frac{\partial H_{scat,y}}{\partial z} = \frac{\varepsilon_o - \varepsilon_{xi}}{\varepsilon_{xi}}E_{inc,x}$$

$$E_{scat,y} - \frac{1}{j\omega\varepsilon_{yz}}\frac{\partial H_{scat,x}}{\partial z} + \frac{1}{j\omega\varepsilon_{yx}}\frac{\partial H_{scat,z}}{\partial x} = \frac{\varepsilon_o - \varepsilon_{yi}}{\varepsilon_{yi}}E_{inc,y} \quad (8)$$

$$E_{scat,z} - \frac{1}{j\omega\varepsilon_{zx}}\frac{\partial H_{scat,y}}{\partial x} + \frac{1}{j\omega\varepsilon_{zy}}\frac{\partial H_{scat,x}}{\partial y} = \frac{\varepsilon_o - \varepsilon_{zi}}{\varepsilon_{zi}}E_{inc,z}.$$

Maxwell's equations are discretized using a Yee cell as shown in Fig. 1 [4]. Therefore, the first step in the construction of the MRFD algorithm is the discretization of the computational space into cells.
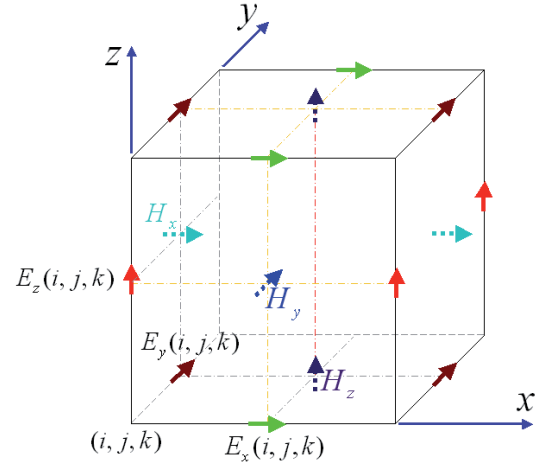

Fig. 1. Yee cell demonstrating the positions of the E and H field vector components within a cubical grid.

In the three-dimensional Yee grid shown in Fig. 1, we apply MRFD approximation method to (7) as follows

$$H_{scat,x}(i,j,k)$$

$$+ \frac{1}{j\omega\mu_{xy}(i,j,k)\Delta y}\sum_{l=1}^{3}a(l)\left[E_{scat,z}(i,j+l,k) - E_{scat,z}(i,j-l+1,k)\right]$$

$$- \frac{1}{j\omega\mu_{xz}(i,j,k)\Delta z}\sum_{l=1}^{3}a(l)\left[E_{scat,y}(i,j,k+l) - E_{scat,y}(i,j,k-l+1)\right]$$

$$= \frac{\mu_o - \mu_{xi}(i,j,k)}{\mu_{xi}(i,j,k)}H_{inc,x}(i,j,k)$$

(9.a)

$$H_{scat,y}(i,j,k)$$

$$+ \frac{1}{j\omega\mu_{yz}(i,j,k)\Delta z}\sum_{l=1}^{3}a(l)\left[E_{scat,x}(i,j,k+l) - E_{scat,x}(i,j,k-l+1)\right]$$

$$- \frac{1}{j\omega\mu_{yx}(i,j,k)\Delta x}\sum_{l=1}^{3}a(l)\left[E_{scat,z}(i+l,j,k) - E_{scat,z}(i-l+1,j,k)\right]$$

$$= \frac{\mu_o - \mu_{yi}(i,j,k)}{\mu_{yi}(i,j,k)}H_{inc,y}(i,j,k)$$

(9.b)

$$H_{scat,z}(i,j,k)$$

$$+ \frac{1}{j\omega\mu_{zx}(i,j,k)\Delta x}\sum_{l=1}^{3}a(l)\left[E_{scat,y}(i+l,j,k) - E_{scat,y}(i-l+1,j,k)\right]$$

$$- \frac{1}{j\omega\mu_{zy}(i,j,k)\Delta y}\sum_{l=1}^{3}a(l)\left[E_{scat,x}(i,j+l,k) - E_{scat,x}(i,j-l+1,k)\right]$$

$$= \frac{\mu_o - \mu_{zi}(i,j,k)}{\mu_{zi}(i,j,k)}H_{inc,z}(i,j,k).$$

(9.c)

Similarly, the MRFD equations representing (8) can be written as

$E_{scat,x}(i,j,k)$

$$-\frac{1}{j\omega\varepsilon_{xy}(i,j,k)\Delta y}\sum_{l=1}^{3}a(l)\big[H_{scat,z}(i,j+l-1,k)-H_{scat,z}(i,j-l,k)\big]$$

$$+\frac{1}{j\omega\varepsilon_{xz}(i,j,k)\Delta z}\sum_{l=1}^{3}a(l)\big[H_{scat,y}(i,j,k+l-1)-H_{scat,y}(i,j,k-l)\big]$$

$$=\frac{\varepsilon_{o}-\varepsilon_{xi}(i,j,k)}{\varepsilon_{xi}(i,j,k)}E_{inc,x}(i,j,k)$$

(10.a)

$E_{scat,y}(i,j,k)$

$$-\frac{1}{j\omega\varepsilon_{yz}(i,j,k)\Delta z}\sum_{l=1}^{3}a(l)\big[H_{scat,x}(i,j,k+l-1)-H_{scat,x}(i,j,k-l)\big]$$

$$+\frac{1}{j\omega\varepsilon_{yx}(i,j,k)\Delta x}\sum_{l=1}^{3}a(l)\big[H_{scat,z}(i+l-1,j,k)-H_{scat,z}(i-l,j,k)\big]$$

$$=\frac{\varepsilon_{o}-\varepsilon_{yi}(i,j,k)}{\varepsilon_{yi}(i,j,k)}E_{inc,y}(i,j,k)$$

(10.b)

$E_{scat,z}(i,j,k)$

$$-\frac{1}{j\omega\varepsilon_{zx}(i,j,k)\Delta x}\sum_{l=1}^{3}a(l)\big[H_{scat,y}(i+l-1,j,k)-H_{scat,y}(i-l,j,k)\big]$$

$$+\frac{1}{j\omega\varepsilon_{zy}(i,j,k)\Delta y}\sum_{l=1}^{3}a(l)\big[H_{scat,x}(i,j+l-1,k)-H_{scat,x}(i,j-l,k)\big]$$

$$=\frac{\varepsilon_{o}-\varepsilon_{zi}(i,j,k)}{\varepsilon_{zi}(i,j,k)}E_{inc,z}(i,j,k).$$

(10.c)

The $a(l)$ coefficients in (9) and (10) are given in Tab. 1.

l	1	2	3
$a(l)$	1.2291667	-0.09375	0.0104167

Tab. 1. $a(l)$ coefficients [11] for the region including the scatterer.

We used FDFD modeling for the PML region to save computation time [1, 4]. Only the region including the scatterer is modeled with MRFD method.

Similar to the FDFD method, the field components for each cell can be computed by solving the linear system of equations (9) and (10). For a problem consisting of N number of Yee cells, these equations can be arranged in a matrix form as $[A][EH] = [F]$ where $[A]$ is a $(6N \times 6N)$ coefficients matrix, $[EH]$ is the unknown vector of size $6N$ containing scattered E and H field components, and $[F]$ is the excitation vector of size $6N$ representing the right hand side of equations (9) and (10), and is a function of all incident field components [4]. Since the coefficient matrix $[A]$ is a highly sparse matrix, to cope with the computer mem-

ory limitations, only non-zero elements are stored while performing the matrix solution. It is very hard to employ direct solution techniques in order to solve such a very large sparse matrix equations. Iterative solvers such as BICGSTAB [14] are usually used in these cases [1, 4]. The numerical results obtained in this study are based on the Fortran code utilizing the "vanilla" version of BiCG-STAB algorithm [4, 15].

3. Numerical Results

A dielectric sphere and a dielectric cube with a relative permittivity (ε_r) of 4 and relative permeability (μ_r) of 1, have been modeled. The diameter of the sphere is set to 30 cm, which is also the dimension of one side of the cube. The scatterers presented in this section are assumed to be illuminated by a θ-polarized plane wave incident from the direction where θ_{inc} is 180° and φ_{inc} is 0°, while the centers of the scatterers are at the origin of the computation space. The bistatic radar cross sections of the scatterers are plotted at E-plane ($\varphi = 0°$ plane). The basic building block for modeling of the structure is a cube cell.

The bistatic radar cross section of the mentioned dielectric sphere at 1 GHz is given in Fig. 2. Since curved surfaces of the scatterers are staircased, in order to have more accuracy on the results, the cube cell size should be decreased. However this can significantly increase the computational memory need of the problem. In Fig. 2, the exact result for $\sigma_{\theta\theta}$ is compared with FDFD simulations using different cell sizes: One side of the cubic cell is chosen to be 0.75 cm, 1 cm, 1.5 cm for three simulations. One can easily notice the improvement in the accuracy with reduced cell size. The bistatic radar cross section $\sigma_{\theta\theta}$ is calculated as

$$\sigma_{\theta\theta} = \lim_{r\to\infty} 4\pi r^2 \frac{\left|E_\theta^{scat}\right|^2}{\left|E_\theta^{inc}\right|^2}$$

(11)

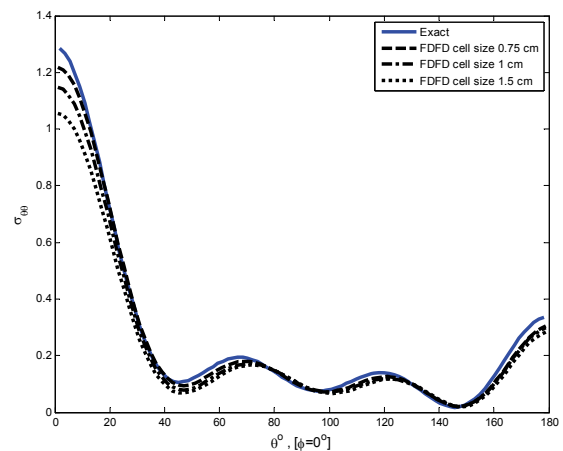where r is the distance from the center of the scatterer [13].

Fig. 2. Radar cross section of dielectric sphere at 1 GHz using FDFD method for different cell sizes.

The scattering of the same sphere is generated using MRFD scheme with cell size of 1.5 cm. The results from FDFD and MRFD simulations with the same cell size are compared with the exact solution in Fig. 3. The accuracy of the MRFD algorithm can easily be seen. Modeling the computational space with the same number of cells, MRFD converges to the exact solution better than FDFD method does.
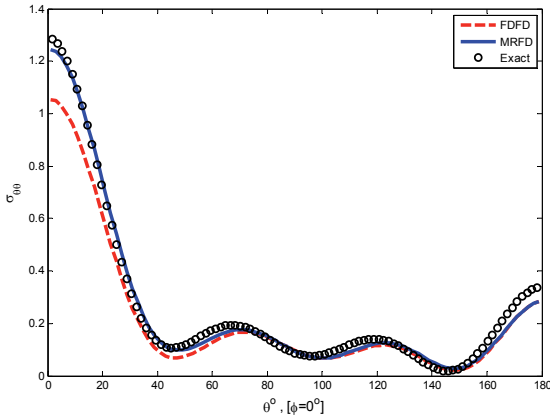

Fig. 3. Radar cross section of dielectric sphere at 1 GHz using FDFD and MRFD methods for the same cell size (one side of the cubic cell is 1.5 cm).

A performance calculation of MRFD and FDFD methods has been performed for dielectric sphere case. The number of nonzero elements in matrix **A**, simulation time, and calculated error percentage values are shown in Tab. 2 along with the cell size for both FDFD and MRFD techniques. The calculation of normalized error value is performed using the formula of

$$error(\%) = \frac{\sum_{i=1}^{N} \left| SR(i\frac{180^0}{N}) - Exact(i\frac{180^0}{N}) \right|}{N \times \left| Exact_{max} \right|} \times 100 \quad .(12)$$

SR and *N* denote the simulation result function obtained from FDFD and MRFD simulations and the number of points where the error difference is calculated, respectively. For the calculation of error, 88 equally spaced number of points are taken from the exact radar cross section data (from 0^0 to 180^0), and used in (11). The angle points to calculate the error percentage are chosen with 2 degrees apart. Since the exact scattering data for the beginning and the last points is not given from the analytic calculating tool, we used 88 points. We could have also chosen more than 88 points.

We can see from Tab. 2 that, regarding the same level of accuracy, the needed memory and simulation time for MRFD modeling dramatically decrease when we compared with those of the FDFD simulation. For example, let us assume 2.12 % error value would be sufficient for us, using FDFD method we could solve the problem in 32.73 minutes, while using MRFD method this time would drop to 3.93 minutes. For this specific level of accuracy the number of unknowns of MRFD method is less than the half

of FDFD method. One can see from Fig. 4 that as the cell size decreases, both FDFD and MRFD converge to a certain error percentage value. The number of nonzero elements is not proportional to the simulation time, because the iterative technique we use needs more number of iterations to converge for bigger matrices. Since the simulation time for each iteration is longer for bigger matrices, we eased the convergence criteria for fine meshes not to wait for very long time for a small amount of improvement in the accuracy.

Method	Cell size [cm]	Number of nonzero elements	Simulation time [min]	Error [%]
FDFD	0.75	6,383,700	73.85	1.15
FDFD	1.00	3,683,250	32.73	2.12
FDFD	1.50	1,877,400	7.93	3.45
FDFD	2.00	1,253,700	3.90	5.93
MRFD	0.75	10,067,940	76.07	1.13
MRFD	1.00	5,330,610	34.55	1.29
MRFD	1.50	2,423,880	9.64	1.57
MRFD	2.00	1,510,740	3.93	2.12

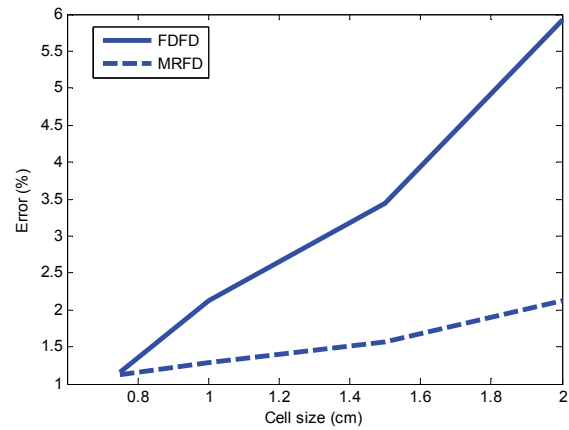**Tab. 2.** Performance comparison of FDFD and MRFD.

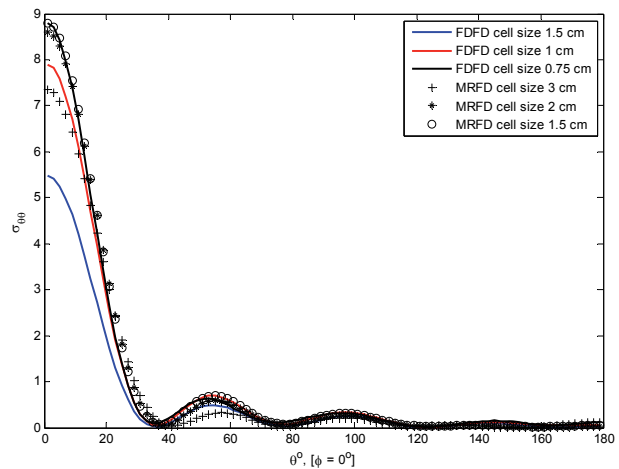**Fig. 4.** The cell size vs. error percentage for FDFD and MRFD simulations given in Tab. 2.

Fig. 5. Radar cross section of dielectric cube at 1 GHz using FDFD and MRFD with different cell sizes.
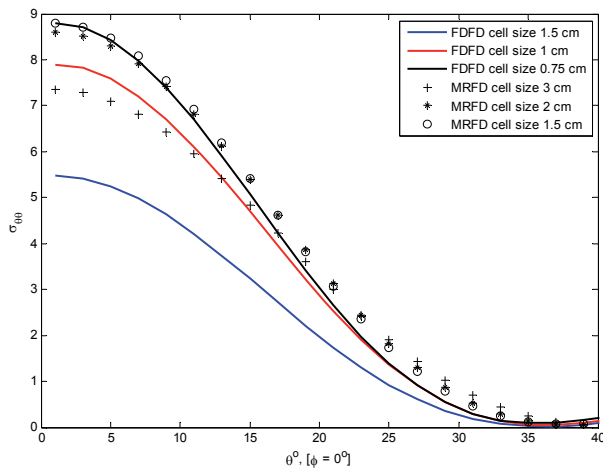
Fig. 6. Radar cross section of dielectric cube at 1 GHz using FDFD and MRFD with different cell sizes. Zoomed in view of Fig. 5.

Fig. 5 and 6 show the bistatic radar cross section of the dielectric cube mentioned before. For this cube modeling, MRFD method can achieve the same level of accuracy with FDFD method using about 2.5 times bigger cubic cells. MRFD with 2 cm cell size simulation provides nearly the same result with FDFD scheme using 0.75 cm cell size. Depending on the simulations we ran, we can say that MRFD method has better performance for dielectric cube modeling, comparing with its performance at sphere case.

4. Conclusions

In this work, the multiresolution frequency domain algorithm for the scattering analysis of three–dimensional arbitrarily shaped dielectric objects is derived and verified. The scattered field approach is successfully implemented into the MRFD formulation. The advantages of this method are validated by comparing the simulation results to those obtained from the analytic computations and FDFD method simulations. The bistatic radar cross section calculations of MRFD are in good agreement in comparison to the exact results and FDFD calculations. Apparently, MRFD method offers advantage for coarse meshes, while for finer meshes the accuracy seems to converge to a level, where for the same mesh size FDFD method demonstrates the similar accuracy. As a disadvantage, MRFD demands more memory and simulation time for fine mesh cases than FDFD does.

Acknowledgements

References

[1] KUZU, L., DEMIR, V., ELSHERBENI, A. Z., ARVAS, E. Electromagnetic scattering from arbitrarily shaped chiral objects using the finite difference frequency domain method. *Progress in Electromagnetics Research*, 2007, vol. 67, p. 1 - 24.

[2] AL SHARKAWY, M. H., DEMIR, V., ELSHERBENI, A. Z. The iterative multi-region algorithm using a hybrid finite difference frequency domain and method of moment techniques. *Progress in Electromagnetics Research*, 2006, vol. 57, p. 19 - 32.

[3] ALKAN, E., DEMIR, V., ELSHERBENI, A. Z., ARVAS, E. Dual-grid finite-difference frequency-domain method for modeling chiral medium. *IEEE Transactions on Antennas and Propagation*, 2010, vol. 58, no. 3, p. 817 - 823.

[4] YAGLI, A. F., GOKTEN, M., IMECI, S. T., KUZU, L. Scattering from gyrotropic bodies using FDFD method. *International Journal of RF and Microwave Computer-Aided Engineering*, 2011, vol. 21, no. 1, p. 77 - 84.

[5] GOKTEN, M., ELSHERBENI, A. Z., ARVAS, E. The multiresolution frequency domain method for general guided wave structures. *Progress in Electromagnetics Research*, 2007, vol. 69, p. 55 – 66.

[6] GOKTEN, M., ELSHERBENI, A. Z., ARVAS, E. A multiresolution frequency domain method using biorthogonal wavelets. In *ACES Conf.* Miami (FL), 2006.

[7] GOKTEN, M., ELSHERBENI, A. Z., ARVAS, E. Electromagnetic scattering analysis using the two-dimensional MRFD formulation. *Progress in Electromagnetics Research*, 2008, vol. 79, p. 387 – 399.

[8] GOKTEN, M., ELSHERBENI, A. Z., YAGLI, A. F. Efficient analysis of two-dimensional RCS scattering analysis using the MRFD technique. In *ACES Conf.* Williamsburg (VA), 2011.

[9] KUNZ, K. S., LUEBBERS, R. J. *The Finite Difference Time Domain Method for Electromagnetics*. Boca Raton: CRC Press LLC, 1993.

[10] BERENGER, J. A perfectly matched layer of the absorption of electromagnetic waves. *J. Comp. Phys.*, 1994, vol. 114, no. 2, p. 185 - 200.

[11] DAUBECHIES, I. *Ten Lectures on Wavelets*. Philadelphia (PA): Society for Industrial and Applied Mathematics, 1992.

[12] YAGLI, A. F., LEE, J. K., ARVAS, E. Scattering from three-dimensional dispersive gyrotropic bodies using the TLM method. *Progress in Electromagnetics Research B*, 2009, vol. 18, p. 225 - 241.

[13] DEMIR, V., ELSHERBENI, A., WORASAWATE, D., ARVAS, E. A graphical user interface (GUI) for plane-wave scattering from a conducting, dielectric, or chiral sphere. *IEEE Antennas and Propagation Magazine*, 2004, vol. 46, no. 5, p. 94 - 99.

[14] VAN DER VORST, H. A. Bi-CGSTAB: A fast and smoothly converging variant of Bi-CG for the solution of nonsymmetric linear systems. *SIAM J. Sci. Stat. Comput.*, 1992, vol. 13, no. 2, p. 631 - 644.

[15] SLEIJPEN, G. L. G., FOKKEMA, D. R. BiCGstab(l) for linear equations involving unsymmetric matrices with complex spectrum. *Electronic Transactions on Numerical Analysis (ETNA)*, 1993, vol. 1, p. 11 – 32.

About Authors ...

Ahmet Fazil YAGLI received the B.S. degree in Electrical and Electronics Engineering from Middle East Technical University, Ankara, Turkey in 2001, and the M.S. and Ph.D. degrees in Electrical Engineering from Syracuse University, Syracuse, NY in 2005 and 2006, respectively. He served as a teaching assistant from August 2001 to May

2002, and as a research assistant from May 2002 to May 2006 at the Electrical Engineering and Computer Science Department of Syracuse University, Syracuse, NY. He is currently working for Turksat AS, Turkish Satellite Operator, in Ankara, Turkey. His research interests are in areas of computational methods for electromagnetics, radar cross section computation, and design and implementation of microwave devices and satellite communications.